James R. Scott (S'80) was born in Melbourne, Australia, in 1957. He received the B.Eng. (communication eng.) degree with distinction and the M.Eng. degree from the Royal Melbourne Institute of Technology in 1979 and 1982, respectively. In 1982 he was also awarded a COMSOC Scholarship by the IEEE Communications Society.

After completing the M.Eng. degree, he worked for a brief period with Consolidated Technology (Aust.) Pty. Ltd. on an *X*-band radar repeater and UHF oscillators. He then joined the Electrical Engineering Department at the University of Melbourne, where he is currently investigating the small and large signal operation of dual-gate GaAs FET's as the basis of a Ph.D. thesis.

His major research interests are in microwave active and passive circuits, the application of dual-gate FET's to optical communication systems, MIC fabrication techniques, and automated microwave measurement techniques.

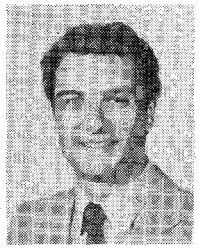

Robert A. Minasian (S'78–M'80) was born in May, 1953. He received the B.E.(Elec.) degree from the University of Melbourne, Australia in 1974. In 1975, he was awarded a United Kingdom Commonwealth Scholarship, and received the M.Sc. degree with distinction from University College, University of London, in 1976. His Ph.D. studies involved research on the large signal operation of microwave MESFET transistors, and he was awarded the Ph.D. degree from the University of Melbourne in 1980. During 1983, he was a Visiting Research Fellow at the Laboratoires d'Electronique et de Physique Appliquée, France.

He is presently a Lecturer in Electrical Engineering at the University of Melbourne, Australia. His current research interests include microwave signal processing circuits, optoelectronic devices, and fiber optic communications.

Dr. Minasian is a senior member of the IREE.

Dual-Gate MESFET Mixers

CHRISTOS TSIRONIS, MEMBER, IEEE, ROMAN MEIERER, AND RAINER STAHLMANN

Abstract—**A theoretical and experimental investigation of dual-gate MESFET mixers is presented. Based on a detailed analysis of the different nonlinear modes of DGFET's, a computer-aided modeling procedure has been developed, which allowed to recognize and optimize critical circuit and bias conditions for high conversion gain and IF bandwidth. Theoretical results are in good agreement with experiments on a 12-GHz TV reception mixer with 8-dB conversion gain and 800-MHz bandwidth.**

I. INTRODUCTION

IN MODERN MICROWAVE superheterodyne receivers, GaAs FET's are used as preamplifiers, local oscillators, and mixers in hybrid [1] or monolithic [2] versions. Both single-gate FET's (SGFET's) and dual-gate FET's (DGFET's) are used as mixers, the last ones even up to *Ka*-band frequencies [3]. The advantages of employing DGFET's as down converters instead of Schottky diodes or SGFET's are, except for conversion gain and reasonable noise figure which are inherent also to SGFET mixers, the intrinsic separation of signal and local oscillator ports and the possibility of separate matching and direct combination of the corresponding powers inside the device. This avoids cumbersome passive couplers and is an important requirement of monolithic circuit designs. The MMIC's DGFET mixers are probably the only adequate solution, as has been shown in the case of *X*-band direct satellite broadcasting receivers [2].

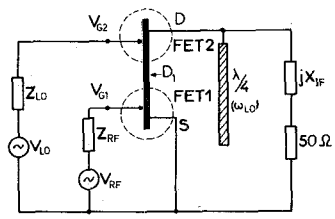

Fig. 1. Principle of DGFET mixer operation.

In spite of the obvious importance of the mixer application of DGFET's, the mixing mechanism of this device is not yet completely understood. This is due to the floating potential of the intergate channel region (D_1 in Fig. 1) strongly dependent on the amplitude of the local oscillator voltage applied onto either of the two gates. The bias and saturation conditions of both FET parts of the DGFET are consequently changing during LO voltage excursion and cause them to act as a mixer, or as RF resp. IF amplifier separately.

This paper deals with computer-aided modeling optimization and testing of DGFET mixers in the three principal mixing modes of practical interest. After an initial general investigation of mixing possibilities with DGFET's, the modeling procedure is described, and examples for two

Manuscript received June 14, 1983; revised December 5, 1983.

C. Tsironis and R. Meierer are with Laboratoires d'Electronique et de Physique Appliquée, 3 Avenue Descartes, 94450 Limeil-Brévannes, France.

R. Stahlmann is with the Institute of Semiconductor Electronics, Technical University of Aachen, West Germany.

0018-9480/84/0300-0248$01.00 ©1984 IEEE

different mixing modes are given. Computed results are compared with MIC mixers, and predictions for a MMIC version are also taken into consideration.

II. The Principle of Dual-Gate FET Mixers

Fig. 1 illustrates the principle of DGFET mixer operation. The signal and local oscillator power are injected into either one of the two gates. Usually, the local oscillator is connected with gate 2 and the signal is injected into gate 1. In this way, a separation of signal and local oscillator power is assured so that well-known techniques for input power and noise matching of gate 1 can be applied. The IF signal is extracted from the drain and fed after reactive matching either to a 50-Ω load or to the input port of a postamplifier. Calculations have shown that the direct power transfer between the IF output of the mixer FET and the input of a postamplifier FET is easier to obtain in the IF frequency band of 1 to 2.7 GHz can be covered, whereas passing through 50 Ω limits the bandwidth to about 800 MHz. However, our circuits have been designed for a 50-Ω load as actually requested for the 12-GHz outdoor receiver unit. For the same reasons, the following frequency bands have been chosen:

Signal band	11.7–12.5 GHz
IF band	0.95–1.75 GHz
Local oscillator frequency	10.75 GHz.

The higher frequencies (f_{LO}, f_{RF}) are short circuited at the drain port using a $\lambda/4$ open microstripline at f_{LO} for the MIC design or a 1-pF interdigitated capacitor being in series resonance at 11 GHz.

The parameters to be adjusted for optimum bandwidth, conversion gain, and noise figure are:

1) the bias voltages V_{G1} and V_{G2} for a given V_{DS};
2) the impedances at all three ports at the main frequency components ω_{RF}, ω_{IF}, ω_{LO}, and the image frequency $\omega_{IM} = 2\omega_{LO} - \omega_{RF}$;
3) the level of the local oscillator power P_{LO}.

III. DGFET Mixer Operation and Modeling

A. The Principal Modes of DGFET Mixer Operation

The main nonlinear operation regions of DGFET's can be identified using its bidimensional transfer characteristic [4] given in Fig. 2. This nomogram can be constructed by inverse overlapping of the dc characteristics of both SGFET parts and taking into account the relations (see Figs. 1 and 2)

$$V_{DS} = V_{D1S} + V_{DD1} \tag{1}$$

$$V_{G2D1} = V_{G2} - V_{D1S}. \tag{2}$$

The vertical traces in Fig. 2 correspond to the external voltage of gate 2 to source, and the internal gate voltages of FET 2 (V_{G2D1}) can be identified on the dotted curves of the nomogram. This diagram furnishes knowledge about the internal potential distribution of the device, especially the critical potential of point D_1 (Fig. 1), as a function of

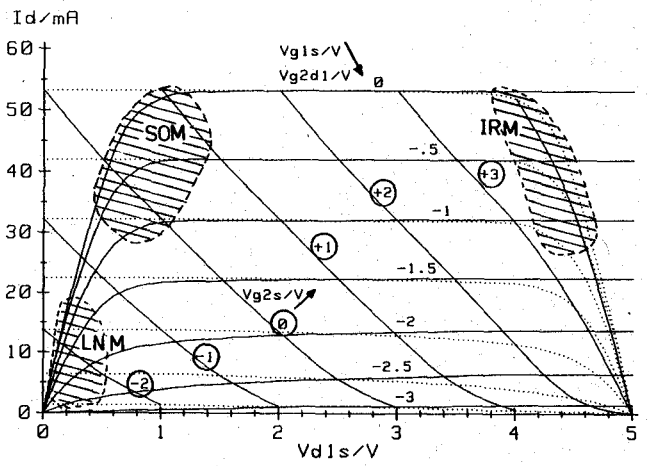

Fig. 2. Transfer characteristic of DGFET (V_{DS} = 5 V).

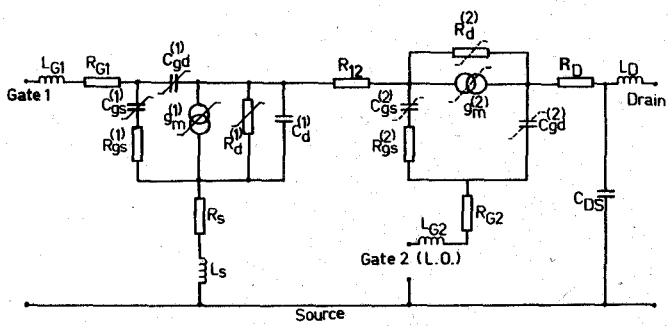

Fig. 3. Equivalent circuit of DGFET indicating the nonlinear elements.

external gate biases for V_{DS} = const. There are mainly three nonlinear regions of the DGFET when pumped by a sinusoidal voltage at gate 2:

1) the low-noise mixer mode (LNM) defined by $V_{G2S} < -1.5$ V (Fig. 2);
2) the self-oscillating mixer mode (SOM) defined by $-0.5\text{ V} < V_{G2S} < +1\text{ V}$ and $-1\text{ V} < V_{G1S}$ (Fig. 2);
3) the image-rejection mixer mode (IRM) defined by $2.5\text{ V} < V_{G2S} < 3.5\text{ V}$ and $-1.5\text{ V} < V_{G1S}$ (Fig. 2).

When the DGFET is driven in one of these three modes, different device parts act nonlinearly causing frequency conversion, whereas other parts act only as RF or IF amplifiers.

We studied the DGFET nonlinear behavior using the nomogram of Fig. 2 and determined equivalent circuit element values from small-signal *S*-parameter measurements for each of the two FET parts and the bias points the device goes through during LO excursion. For that purpose, the quasistatic analysis using Fig. 2 is valid since the LO voltage is supposed to be short circuited at the output of the device.

Fig. 3 is an equivalent circuit of the DGFET showing the elements considered to be in nonlinear operation in the LNM and SOM bias regions (marked with continuous bars) and those elements being nonlinear in the IRM mode (marked with dotted bars).

It is obvious that in the case of LNM and SOM bias regions, mixing takes place inside of FET 1, while FET 2

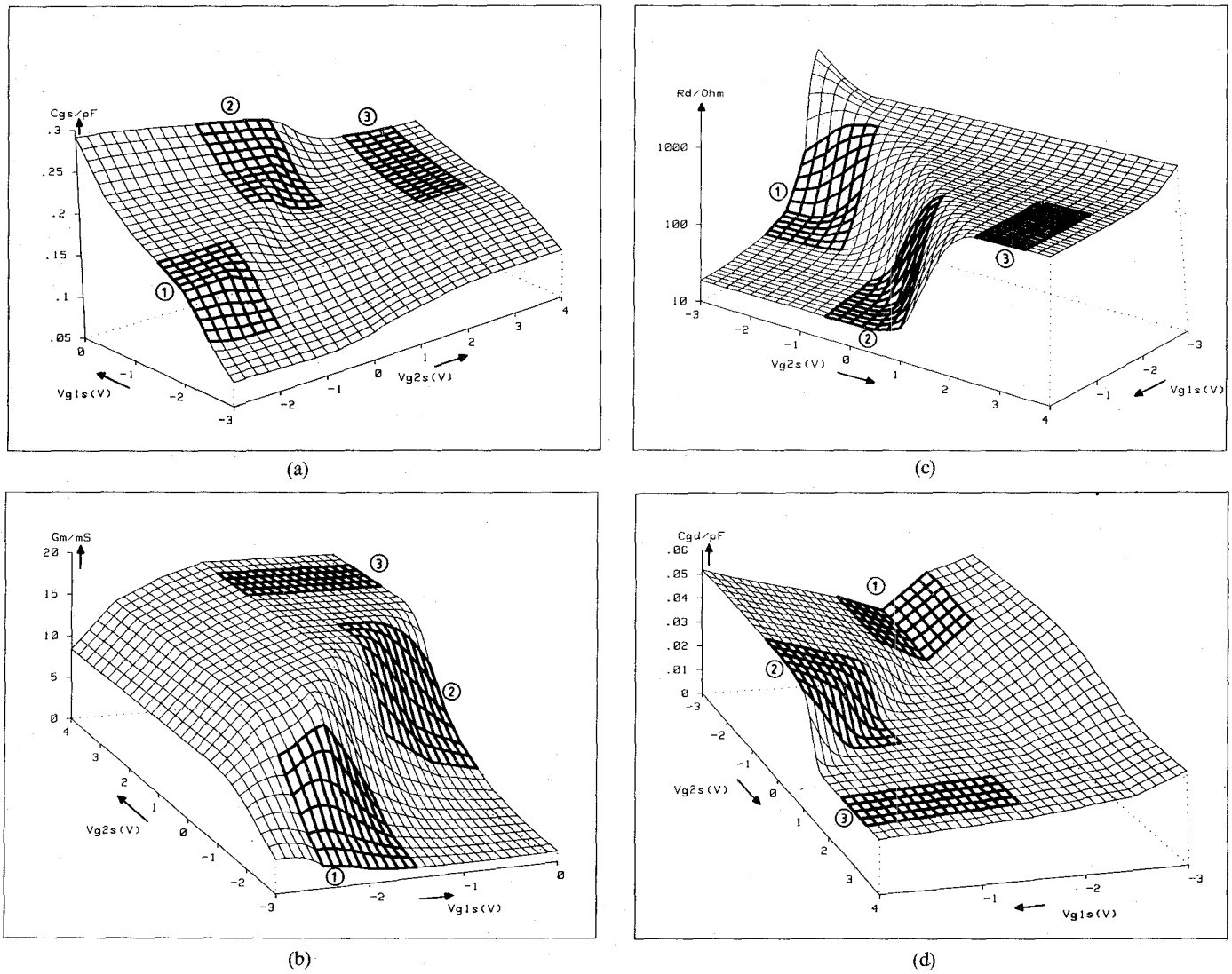

Fig. 4. Variation of the element values of FET 1 ($V_{DS} = 5$ V). ① Low-noise mixer. ② Self-oscillating mixer. ③ Image-rejection mixer. (a) C_{gs}/pF of FET 1. (b) G_m/ms of FET 1. (c) R_d/Ω of FET 1. (d) C_{gd}/pF of FET 1.

acts mainly as an IF postamplifier. In the IRM operation region, FET 1 acts as an RF preamplifier and FET 2 as a mixer.

The variations of the element values of both FET's (Fig. 3) with external bias V_{G1S}, V_{G2S} are clearly described by using the bidimensional representation of Figs. 4 and 5. The values of the elements of the equivalent circuit are determined from medium frequency (500 MHz to 1 GHz) S-parameter measurements and simulations on SGFET's of the same type as the DGFET parts as a function of bias conditions. If such SGFET's are not available, a dc deembedding technique can be applied as described in [7, ch. c, p. 248]. In Fig. 4, the four nonlinear elements of FET 1 are given, whereas Fig. 5 deals with those elements of FET 2.

Also, these diagrams serve to visualize the excursions on the characteristics and the expected parameter nonlinearities caused by the local oscillator as marked in Figs. 4 and 5 by the thicker lines. In the case of pumping into gate 2, the bias point shifts along the V_{G2S} axis.

Mixing nonlinearities with the LO injected into gate 1 can also easily be predicted by using these diagrams and would correspond to a deplacement along the V_{G1S} axis.

The interdependence of the internal bias voltage V_{D1S} on V_{G1S} and V_{G2S} has been derived from Fig. 2 and is included implicitly in the context of Figs. 4 and 5. In Fig. 6, a further classification of the bias swing of the DGFET and especially the saturation mode of the partial FET's 1 and 2 is illustrated.

The mixing operation modes of DGFET's can therefore be summed up as given in Table I.

The properties of the principal operation modes of DGFET mixers can be summarized as follows.

a) In the *low-noise mixer* mode, the main nonlinearities are situated within the FET 1 device part. As can be seen from Fig. 4, the FET 1 transconductance $g_m^{(1)}$ and channel resistance $R_d^{(1)}$ are the important nonlinear elements. Mixing by the nonlinearity of input capacitance $C_{gs}^{(1)}$ and $C_{gd}^{(1)}$ has also been taken into account but is negligible. Since mixing takes place before FET 2, this last one only amplifies the generated IF band. Due to the low device current, the noise figure is found to be favorable. Normally, DGFET's are being employed in this operation area in

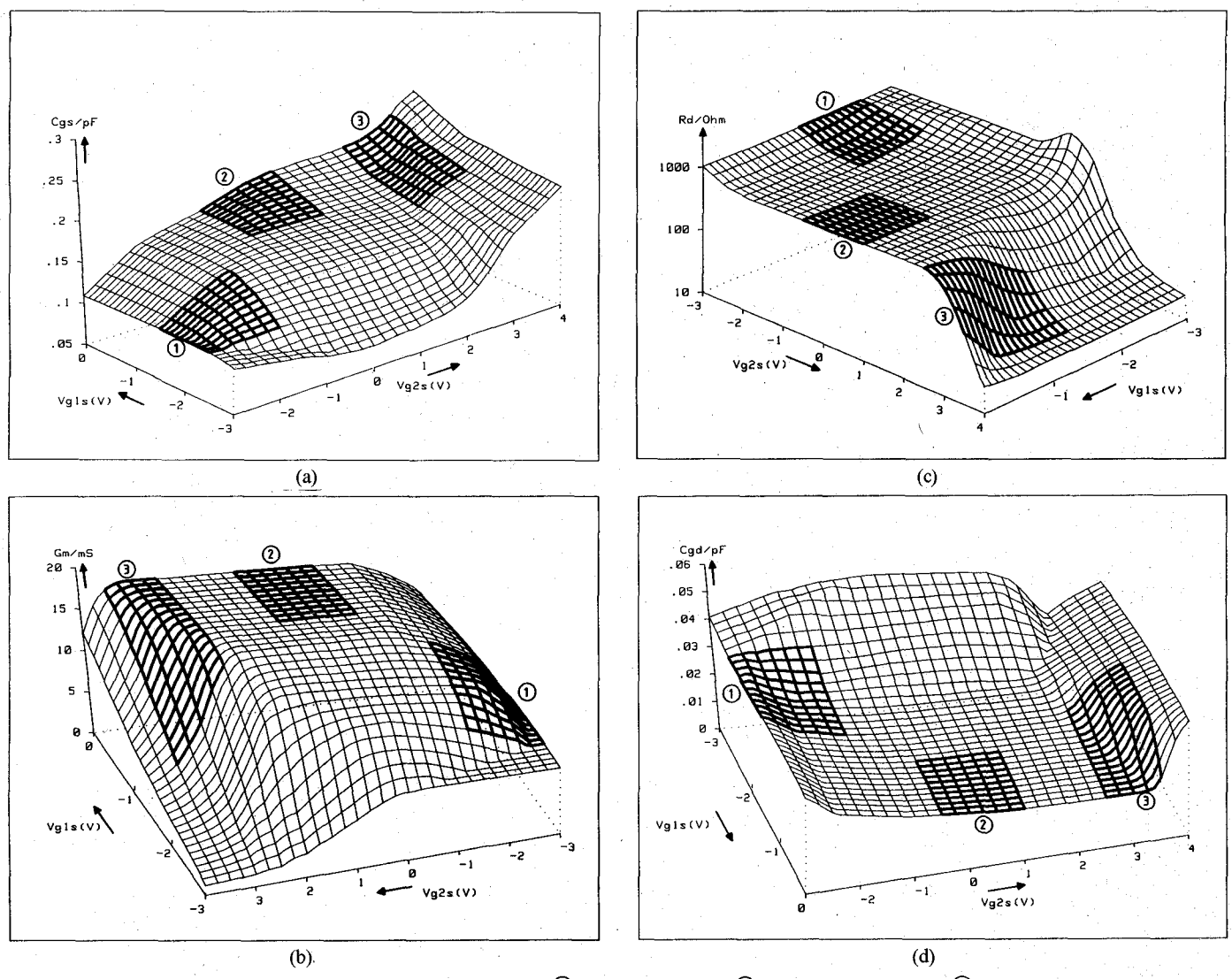

Fig. 5. Variation of the element values of FET 2. ① Low-noise mixer. ② Self-oscillating mixer. ③ Image-rejection mixer. (a) C_{gs}/pF of FET 2. (b) G_m/ms of FET 2. (c) R_d/Ω of FET 2. (d) C_{gd}/pF of FET 2.

TABLE I
REVIEW OF MIXER OPERATION OF DGFET'S

Operation region (ref. Fig. 2)	LNM $V_{G2S} < -1.5$ V	SOM -0.5 V $< V_{G2S} < +1$ V, -1 V $< V_{G1S}$	IRM 2.5 V $< V_{G2S} < 3.5$ V, -1.5 V $< V_{G1S}$
FET 1:	Mixer	Mixer	RF-Amplifier
FET 2:	IF-Amplifier	IF-Amplifier	Mixer
Application	Low-Noise Mixer	Self-Oscillating Mixer	Image Rejection Mixer

order to obtain low-noise performance.

b) In the *self-oscillating mixer* mode, the nonlinearities are of the same type as in the LNM mode, except that now the channel resistance $R_d^{(1)}$ beats more and the transconductance $g_m^{(1)}$ less than before. Here, FET 2 figures also as an IF postamplifier. As can be recognized from Figs. 4 and 5, the transconductances of both FET's now have higher values as in the LNM case. This allows the device to be potentially unstable in the X-band. This effect can be utilized to tune the DGFET as an oscillator and employ it as a self-oscillating mixer [5]. Since the oscillation amplitude is limited by the inherent saturation mechanism, nonlinear operation is assured, and an RF signal introduced into gate 1 is mixed down by the oscillating DGFET. Since the dc current is high-noise performance, it is worse than in the LNM case.

c) For *image-rejection mixer* operation, a modified type of DGFET has to be used. This particular device, the BRFET [6], is fundamentally a DGFET and has been developed at Laboratoires d'Electronique et de Physique Appliquée for use as an active image-rejection filter in 12-GHz TV reception (the image frequency band (9–9.8

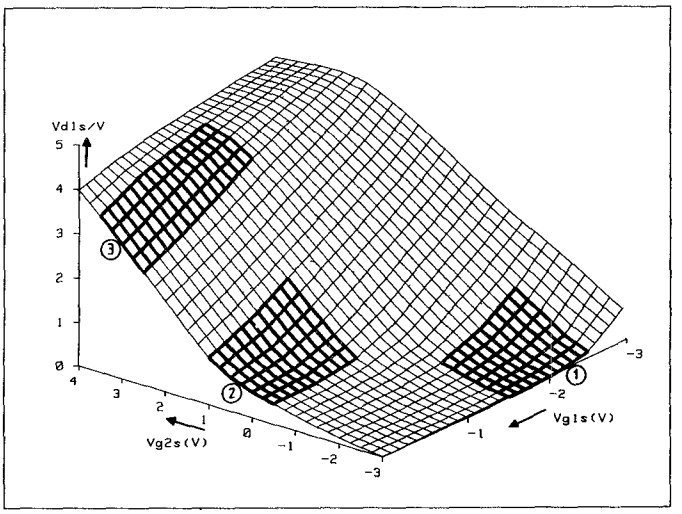

Fig. 6. Internal voltage V_{D1S} of FET 1 ($V_{DS} = 5$ V).

GHz) is suppressed in front of FET 2 by an appropriate integrated LC series resonant circuit placed between the two gates). If the BRFET operates as a mixer in the IRM mode, the nonlinearities are located at FET 2 as can be seen from Figs. 4 and 5 ($g_m^{(2)}, R_d^{(2)}, C_{gs}^{(2)}$). FET 1 acts now as a preamplifier, and mixing takes place inside of FET 2 physically behind the image-rejection filter.

B. Computer-Aided Modeling of DGFET Mixers

The basic assumptions on which the proposed modeling procedure is based are as follows.

1) The local oscillator waveform on the gate 2 is purely sinusoidal. Calculations taking "clipping" into account have shown some degradation of minor importance on conversion gain, as far as the clipping of the LO voltage remains less than 25 percent.

2) Interactions of higher order than direct conversion to IF are neglected.

3) ω_{IF} is small in comparison to ω_{LO}.

4) At the present time, we cannot model the influence of the image frequency ($\omega_{IM} = 2\omega_{LO} - \omega_{RF}$).

After initial identification, using the bidimensional transfer characteristics (Fig. 2), of the nonlinear region on which modeling will be made, the bias point excursion of both FET parts during the local oscillator swing has to be defined more precisely (quasi-static approach). In Fig. 2, it can easily be recognized that either the gate and the drain voltages of both FET parts change more or less sensitively during LO pumping.

For an ensemble of bias points corresponding to this excursion on the characteristics, we measured at lower frequencies (0.5–2 GHz) scattering parameters of the two FET's that compose the DGFET. This can be done either by measuring real SGFET's of the same geometry as the DGFET parts, if available, or by driving one of the two partial FET's of the DGFET into the ohmic region and measuring S-parameters of the other FET following the method described in [7].

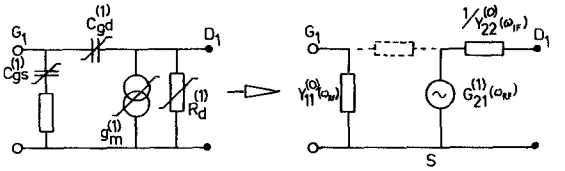

Fig. 7. Schematic of the harmonic analysis procedure of the mixing FET part.

From the obtained set of S-parameters, then, the variation of small-signal element values of a simplified equivalent circuit have been calculated as they are represented in Figs. 4 and 5. These data have then been introduced in matrix form with the interpolation possibility between two successive points into a HP 9836 desk top computer as

$$P_i = P_i(V_{G1S}, V_{G2S}, V_{D1S})$$

where P_i stands for any of the parameters $C_{gs}^{(1)}, C_{gs}^{(2)}$, $g_m^{(1)}, g_m^{(2)}, R_d^{(1)}, \cdots$, and could be reduced to a bidimensional form

$$P_i = P_i(V_{G1S}, V_{G2S})$$

by using the relation

$$V_{D1S} = V_{D1S}(V_{G1S}, V_{G2S})$$

which is visualized in Fig. 6. The variable FET parameters used in our approach in matrix data form can also be calculated using dc modeling of the DGFET. This procedure has been developed at the Institute of Semiconductor Electronics of the Technical University of Aachen, West Germany, tested and found equivalent, but should not be employed before a faster computer is available.

With the data files of the bias-dependent FET parameters, optimum software for compatible circuit analysis, and HP 9836, the mixer behavior and matching circuits at RF, LO, and IF frequencies of gate 1, gate 2, and drain ports have been calculated by using the following steps.

1) Transferal of the sinusoidal local oscillator pumping voltage $V_{G2} = V_{G20} + V_0 \cdot \cos(\omega_{LO} t)$ through the nonlinearity voltage characteristic to obtain Y-parameter variation with time.

2) Harmonic analysis at local oscillator frequency ω_{LO} of the following parameters of the nonlinear FET part:

- $Y_{11}(\omega_{RF})$ in order to obtain the mean value of the input admittance $Y_{11}^{(0)}(\omega_{RF})$,[1]
- $Y_{22}(\omega_{IF})$ in order to obtain the mean value of the output admittance $Y_{22}^{(0)}(\omega_{IF})$,
- $G_{21}(\omega_{RF})$ in order to obtain the equivalent open-circuit voltage conversion gain $G_{21}^{(1)}(\omega_{RF})$ of the mixing FET part.

This last operation, by using G_{21} instead of Y_{21}, allows the modeling of mixing effects not only due to the nonlinear transconductance g_m of the mixing FET but also due to the nonlinear channel resistance R_d, as is shown in Fig. 7.

[1] $Y_{ij}^{(n)}(\omega_k)$ is the nth harmonic of the ijth complex admittance at frequency ω_k.

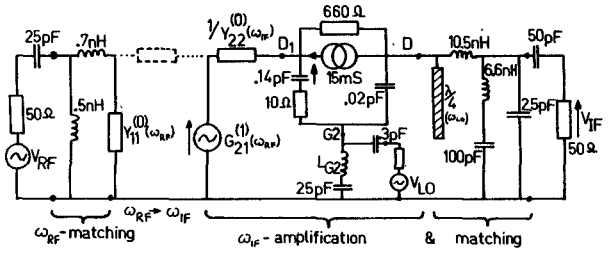

Fig. 8. Equivalent circuit for low-noise mixer modeling.

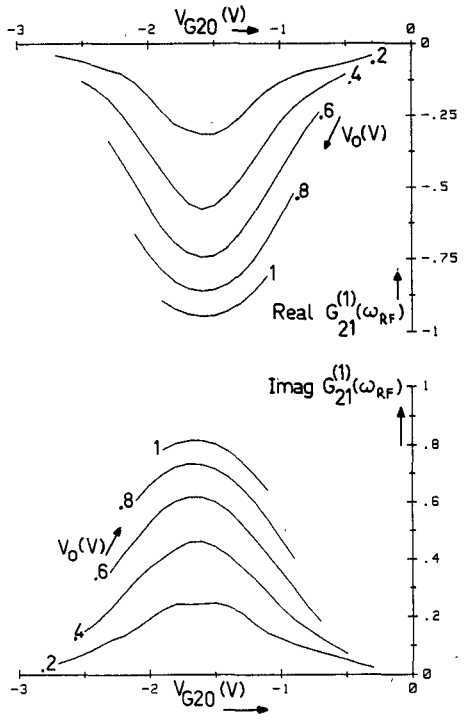

Fig. 9. Calculated open-circuit voltage conversion gain $G_{21}^{(1)}(\omega_{RF})$ of the mixing FET part as a function of gate 2 bias and local oscillator amplitude.

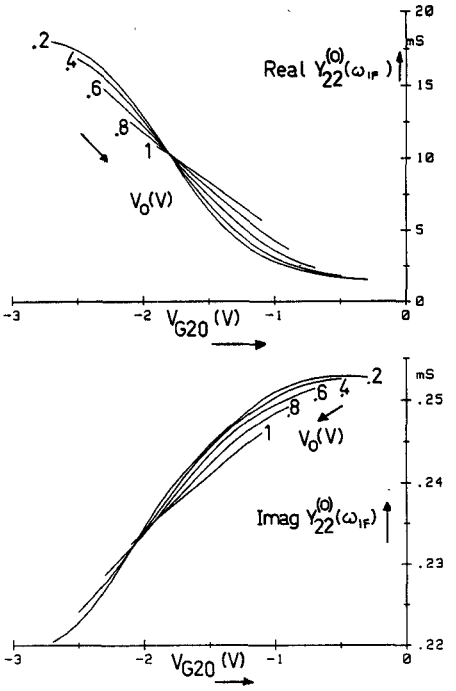

Fig. 10. Calculated output admittance $Y_{22}^{(0)}(\omega_{IF})$ as a function of gate 2 bias and local oscillator amplitude.

3) RF input matching: the mean value of the input admittance $Y_{11}^{(0)}(\omega_{RF})$ at gate 1 is used for conjugate input matching (compare Fig. 8) easily attainable for the required bandwidth (800 MHz at 12 GHz for 12-GHz TV).

4) Interactive optimization of $G_{21}(\omega_{RF})$ nonlinearities as a function of the gate 2 loading impedance.

5)The mixer output impedance at ω_{IF} at the drain, calculated from the circuit in Fig. 8, where $G_{21}^{(1)}(\omega_{RF})$, $Y_{22}^{(0)}(\omega_{IF})$ represent the mixing FET 1, is matched to the 50-Ω load via the IF filter (Fig. 13) for maximum flat gain over the 800-MHz IF bandwidth.

6) If necessary, readjusting of the gate 2 impedance for maximum G_{21} nonlinearity *and* maximum gain of FET 2 (in the cases LNM and SOM).

This rather tedious procedure exists now in the form of a computer program including small-signal circuit analysis facilities and graphics. Fourier analysis has to be loaded supplementarily as well as the element values data.

C. Modeling Results

Fig. 8 shows the small-signal equivalent circuit of a DGFET mixer, as presented here, in the LNM modes. As already discussed in Section III-A, FET 2 acts here as an IF-band postamplifier, whereas mixing mainly occurs within FET 1. Also, as has been pointed out before, the gate 2 impedance has to be considered mainly at two frequencies, the local oscillator frequency ω_{LO} and the IF frequencies ω_{IF}; since it has a double action

1) it has an important influence on the nonlinearity of FET 1 by defining:
   a) the transfer of pumping power from the local oscillator into the mixer,
   b) the input impedance at ω_{LO} of FET 2 which shunts the output of FET 1; and
2) it defines the gain of the IF postamplifying FET 2.

The most important nonlinear fourpole parameters are $G_{21}^{(1)}(\omega_{RF})$ and $Y_{22}^{(0)}(\omega_{IF})$. Figs. 9 and 10 give two examples of variation of real and imaginary parts of these parameters as a function dc bias and local oscillator voltage amplitude for the LNM mode. In our modeling, a first interactive optimization has been made using this type of diagram for best bias choice.

Some of the obtained modeling results using the described procedure are presented below.

The influence of local oscillator power on conversion gain is shown in Fig. 11. The curve is calculated for optimum flat gain over 800-MHz IF bandwidth. A comparison between LNM and SOM modes shows that at SOM a slightly higher LO power is necessary in order to

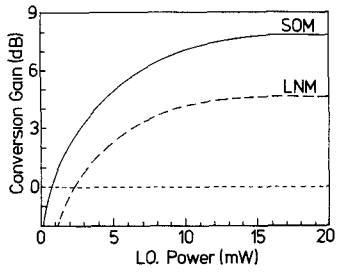

Fig. 11. Calculated conversion gain as a function of LO power (800-MHz bandwidth).

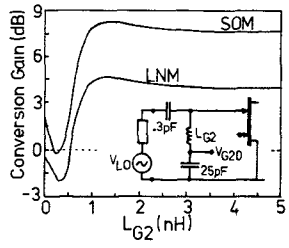

Fig. 12. Influence of the inductive load at gate 2 on the conversion gain.

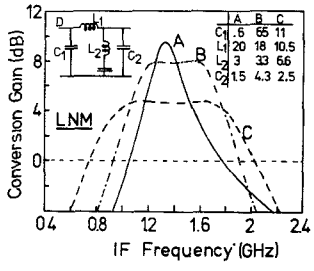

Fig. 13. Influence of the IF matching circuit on the conversion gain and the IF bandwidth.

drive into the optimum gain point. The lower power needed at LNM is related to the fact that both FET's here are near to pinchoff (compare Fig. 2).

The influence of the value of the inductive load at gate 2 is shown in Fig. 12. For values of this inductance higher than a critical minimum of about 1 nH, the conversion gain in both nonlinear modes LNM and SOM is quite constant. The available bandwidth is also maintained as far as the inductance surpasses the mentioned minimum value as is indicated in Fig. 12. These modeling results correspond well with the experimental finding that DGFET's are well suitable as self-oscillating mixers [5], since the inductive load at gate 2 assures simultaneously the oscillation conditions at X-band and a sufficient bandwidth at IF.

The IF matching circuitry is evidently very important concerning the bandwidth of the circuit. As Fig. 13 shows, a bandwidth of around 800 MHz at 4.5-dB conversion gain can be covered for the LNM mode, but higher gain of 8 dB at 400 MHz or even 10 dB at small bandwidths should also be attainable. Experiments show, however, that in the last case the device risks oscillating at frequencies in the IF band.

Finally, an important result of the modeling procedure is the potential bandwidth of a mixer postamplifier version of the circuit, without passing through a 50-Ω reference impedance. As can be seen from Fig. 14, not only the gain of the postamplifier stage is added to the conversion gain of the mixer, but also the bandwidth of the mixer is increased by a factor of about 2. This result should be expected even without complicated modeling since bandwidth is always increased if matching takes place between impedances of similar levels, such as the output of the DGFET mixer and the input of the postamplifying FET.

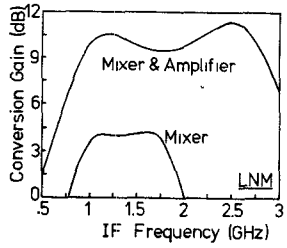

Fig. 14. Calculated conversion gain of a monolithic mixer postamplifier circuit versus IF frequency.

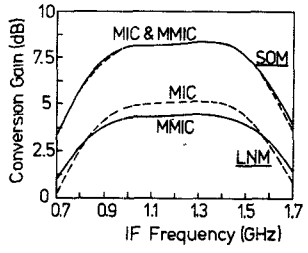

Fig. 15. Calculated conversion gain of the monolithic DGFET mixer (MMIC) compared with the MIC version.

IV. Results and Discussion

DGFET mixers have been designed at 12 GHz with a local oscillator of 10.75 GHz and realized in hybrid form on Al_2O_3 substrates for operation in all three nonlinear modes. In the IRM mode, a BRFET [6] instead of a DGFET has been employed. Its nonlinear behavior is the same as that of a DGFET. Obtained results using DGFET's of L.E.P. with two equal gates of 0.8 μm$\times$150 μm can be summed up as follows.

Low-noise mixer mode: Fig. 8 describes in detail the realized LNM circuit. All matching elements are easily monolithically integrable. This allows us to predict the conversion gain and bandwidth behavior of a monolithic GaAs DGFET mixer in the LNM and SOM modes using the obtained results of the MIC versions of the mixers, as can be seen in Fig. 15. Spiral inductors, interdigital, and MIM capacitors have been used for modeling the MMIC mixer. The $\lambda/4$ open microstripline for RF and LO suppression at the drain has been replaced by an interdigital capacitor with a series resonance at 11 GHz. The optimum Z_2 for best conversion gain and IF bandwidth is a pure inductance, as Fig. 12 shows. However, the size of the decoupling capacitor (0.3 pF) has to be carefully chosen since small values would degrade the efficiency of the LO, but higher values would shunt and cancel the effect of the inductance L_{G2}. The conversion gain of that mixer is given in Fig. 16: it is compared with modeling results obtained

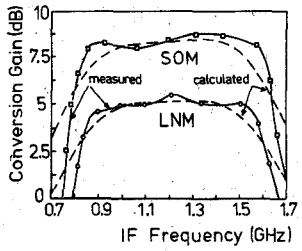

Fig. 16. Measured and calculated conversion gain of the DGFET mixer in the LNM and SOM mode.

according to the already described procedure. A close agreement of experimental and modeled values can be stated. The SSB noise figure has been measured in the 800–1500-MHz IF range using an automatic noise analyzer, and it was of the order of 8–9 dB. No predictions on the noise figure of DGFET mixers can yet be made using our modeling procedure, but due to the lower dc current in the LNM mode, the best noise figure is expected in this region.

Fig. 16 also gives measured and calculated results of the DGFET in the self-oscillating mixer mode: Due to the higher current and the fact that FET 1 is now in the saturated region (Fig. 2), the DGFET can oscillate if an appropriate purely inductive load at gate 2 is presented. However, the presented experimental and theoretical results of 8-dB conversion gain over the 800-MHz bandwidth are obtained using an external local oscillator at gate 2. The noise figure is in this case higher (10–12 dB).

DGFET mixers in the image-rejection mode employing a BRFET [6] are much more difficult to tune at the IF port due to the sensitivity of the output impedance to LO power (Fig. 2). However, as has been shown in [6], a conversion gain of 4–6 dB and an associated noise figure of 12–13 dB over the 100-MHz bandwidth could be obtained. The corresponding image band (9.5 GHz) rejection was around 30 dB. Due to these difficulties in the realization of IRM circuits, the immediate application of BRFET's is seen in image-rejection amplifiers.

V. Conclusion

A computer-aided modeling and design procedure of DGFET mixers has been presented.

The three principal modes of operation, low-noise mixer, self-oscillating mixer, and image-rejection mixer, have been identified and modeled, and corresponding circuits have been realized.

DGFET mixers for 12-GHz DBS TV with 5-dB conversion gain and 8–9-dB noise figure or 8-dB conversion gain and 10–12-dB noise figure over 800 MHz are presented.

Theoretical performances of MIC and MMIC DGFET mixers are compared and monolithic mixers have been designed.

Acknowledgment

We would like to acknowledge A. Villegas-Danies for his technical assistance, R. A. Minasian from the University of Melbourne for critical discussions, and our colleagues at L.E.P. who furnished the Dual Gate FETs.

References

[1] R. Dessert, P. Harrop, and T. Vlek, "All FET front-end for 12 GHz satellite broadcasting reception," in *Proc. 8th Eur. Microwaves Conf.*, (Paris), 1978, pp. 638–643.

[2] C. Kermarrec, P. Harrop, C. Tsironis, and J. Faguet, "Monolithic circuits for 12-GHz DBS reception," in *1982 IEEE MMIC Symp. Dig.*, (Dallas, TX), pp. 5–10.

[3] E. Watkins, J. M. Schellenberg, and H. Yamasaki, "A 30 GHz receiver," in *1982 IEEE MTTS Symp. Dig.*, (Dallas, TX), pp. 16–18.

[4] C. Tsironis and R. Meierer, "DC characteristics aid dual-gate FET analysis," *Microwaves*, pp. 71–73, July 1981.

[5] C. Tsironis, "12 GHz receiver with self-oscillating dual gate MESFET mixer," *Electron Lett.*, vol. 17, pp. 617–618, 1981.

[6] C. Tsironis, "BRFET: A band rejection FET for amplifier and mixer applications," in *1982 IEEE MTT-S Int. Symp. Dig.*, (Dallas, TX), pp. 271–273.

[7] C. Tsironis and R. Meierer, "Microwave wideband model of GaAs dual gate MESFETs," *IEEE Trans. Microwave Theory Tech.*, vol. MTT-30, pp. 243–251, 1982.

Christos Tsironis (M'81) was born in Athens in 1948. He received the Dipl. Ing. degree in electrical engineering from the University of Karlsruhe, Germany, in 1972, and the Dr. Ing. degree from the Technical University of Aachen, Germany, in 1977.

From 1973 to 1980, he had been with the Institute of Semiconductor Electronics of the Aachen Technical University, where he worked on noise, RF-characterization and modeling, and breakdown behavior of GaAs FET's. In 1980, he joined L.E.P. (Philips Research Laboratories in France) near Paris, where he is involved with work on FET dielectrically stabilized oscillators, YIG oscillators, and dual-gate FET modeling and nonlinear applications. Presently, he is group leader for microwave MIC and MMIC subassemblies at L.E.P. and is also responsible for development of YIG oscillators and DRO's at RTC-Limeil.

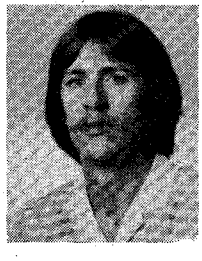

Roman Meierer was born in Kesten, West Germany, in March 1956. From October 1975 to February 1982, he was a student of electrical engineering at the Technical University of Aachen, West Germany. From October 1980 to January 1981 and from March 1982 to August 1982, he completed industrial training periods at the Laboratoires d'Electronique et de Physique Appliquée (L.E.P.) in France. Since October 1982, he has been a member of the technical staff in this laboratory and works on dual-gate FET modeling, YIG oscillators, and on the development of CAD-software.

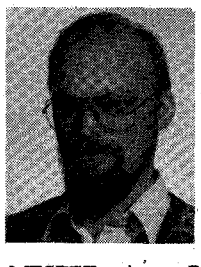

Rainer Stahlmann was born in Bielefeld, West Germany, on September 27, 1947. He received the Dipl.-Ing. degree from the Technical University of Aachen, West Germany, in 1972.

In 1972, he joined the Institute of Semiconductor Electronics, the Technical University of Aachen, working on semiconductor device applications and RF measurements. From October 1981 to March 1982, he worked at the Laboratoires d'Electronique et de Physique Appliquée (L.E.P.) in France on modeling of MESFET mixers. Presently, he is engaged in development of CAD software of microwave integrated circuits.